A GRU-based ensemble learning method for time-variant uncertain structural response analysis

Kun Zhang[1], Ning Chen[1, *], Jian Liu[1], Michael Beer[2,3,4]

[1]State Key Laboratory of Advanced Design and Manufacturing for Vehicle Body, Hunan University, Changsha 410082, China

[2]Institute for Risk and Reliability, Leibniz Universität Hannover, Callinstr. 34, Hannover, Germany

[3]Institute for Risk and Uncertainty, University of Liverpool, Peach Street, L69 7ZF Liverpool, United Kingdom

[4]International Joint Research Centre for Engineering Reliability and Stochastic Mechanics, Tongji University, Shanghai 200092, China

Abstract: Owing to the influence of manufacturing and assembly errors, material performance degradation, external loads and unpredictability of the environment during service, structural response analysis should consider the time-invariant uncertainties and time-variant uncertainties simultaneously. In this paper, a mixed uncertainty model with random variable and stochastic process is adopted to handle this issue. A time-variant uncertain structural response analysis method is proposed based on recurrent neural network using gated recurrent units (GRU) combined with ensemble learning. In the proposed method, by performing Latin hypercube sampling (LHS) of random

variables, multiple GRU networks can be trained to estimate the time-variant system response under fixed random variables. During the process of training GRU models, an active learning strategy is developed and applied to improve model accuracy and reduce training samples. On this basis, a set of augmented data is generated using the trained GRU models. Then the mapping relationship between random variables and structural responses through the Gaussian process (GP) regression is built accordingly. Eventually, the global surrogate model of time-variant uncertain structural response can be obtained by integrating the GRU networks and the GP models. Two numerical examples are used to demonstrate the effectiveness and accuracy of the proposed method. The results indicate that the proposed method can effectively calculate the expectation and standard deviation of the system response under the mixed uncertainty model with random variables and stochastic processes. In addition, it has higher computational efficiency under the premise of ensuring the calculation accuracy.

Keywords: GRU, time-variant response, active learning, Gaussian process, ensemble learning

1.Introduction

Traditional response analysis and optimization of structures are generally based on deterministic parameters. However, it is inevitable that uncertainties exist in practical engineering problems. The uncertainties are mainly deriving from two aspects. One is that the environmental load of the engineering structure is generally random, such as sea waves, earthquakes and wind force. The other is, due to the incomplete controllability of measurement and manufacturing accuracy, there are uncertainties

existing in the structure itself. Thus, considering the randomness of the external load and the uncertainty existing in the model simultaneously during the structural response analysis process deserves the attention of researchers to obtain results with valued engineering application. Regardless of these ubiquitous uncertainties and treating them as deterministic information, the response prediction and the optimal design of a structure may fail.

For uncertainty analysis, when enough sample data can be obtained, time-invariant stochastic model and time-variant stochastic model are two ideal non-deterministic mathematical models. The time-invariant stochastic model is developed for time-independent uncertain parameters, and is the most widely used uncertain model by far. The stochastic perturbation method is a popular method [1,2,3]. In engineering practice, the first-order and second-order truncated expansion of Taylor series are usually used, and the solutions considering higher-order will become very complicated. Therefore, the stochastic perturbation method is generally only applicable to random problems with small-scale variation, which is its inherent defect. The spectral stochastic method is another effective stochastic numerical analysis method [4,5,6]. The advantage of the spectral stochastic method is that it can obtain the expectation, variance and probability density function of the random response at the same time. However, the computational accuracy of the spectral stochastic method increases with the increase of the number of chaotic polynomial terms, but the computational efficiency decreases [7,8]. Therefore, the spectral stochastic method is mainly used to solve random problems with small degrees of freedom. The Monte Carlo method is a

simple and robust approach to deal with the random structural response analysis [9,10,11,12, 13]. Its obvious shortcoming lies in the problem of convergence rate. In order to obtain reliable calculation results, a huge number of samples is required. In order to solve this problem, researchers have proposed several fast Monte Carlo sampling methods, including important sampling method [14, 15], line sampling method [16] and control-variable Monte Carlo method [17, 18]. The time-variant stochastic model is an effective mathematical model for dealing with time-variant uncertainties. Shinozuka et al. used the homogeneous stochastic oscillation process to analyze the power spectrum under multi-dimensional excitation [19]. Cho et al. simulated multi-correlated non-stationary stochastic processes by Karhunen–Loève expansion [20]. Kim et al. modeled non-Gaussian and non-stationary random processes using Karhunen–Loève expansion and iterative translation approximation method [21]. Grigoriu et al. studied the accuracy of polynomial chaos expansion of non-Gaussian random processes [22]. Mao et al. proposed a non-stationary random process representation method based on Hilbert spectrum [23].

Due to the complexity of practical engineering problems, multiple types of uncertainties may exist simultaneously. Elishakoff and Colombi used mixed random and interval models for the uncertain structural response analysis under random excitations, and used anti-optimization technology to find the least favorable values of the mean square response [24]. Wang et al. proposed a stochastic interval finite volume method to predict the steady-state temperature field with hybrid random and interval uncertainties [25]. Wang et al. presented a reliability-based topology optimization for

heterogeneous composite structures under interval and convex mixed uncertainties [26]. Xia et al. proposed a hybrid probabilistic interval perturbation methods for structural–acoustic problem with random and interval variables [27]. Chen et al. introduced a bounded hybrid uncertain model with interval variable and bounded random variable for the response analysis of the composite structure-acoustic system [28]. Zhu et al. proposed a probability-box-based method for propagation of multiple types of epistemic uncertainties [29]. In the researches mentioned above, the time-variant characteristics of the uncertain parameters are not considered in the hybrid uncertain models. Whereas, owing to the influence of material performance degradation, external loads and unpredictability of the environment during service, the uncertain parameters in the structure system may be time-dependent. Up to now, the uncertain response analysis of the structure system involving a mixture of stochastic variables and stochastic processes has seldom been investigated.

In addition, most of current approaches for time-variant uncertain problems rely on sampling-based methods and analytical approximation methods, which may cause a fatally computational burden [30,31]. However, to the best of our knowledge, using deep learning to build surrogate models has not been widely used in the response analysis of structures with time-variant uncertainties. While other works in the field of time-dependent reliability analysis have demonstrated the potential of deep learning models [32,33]. Zhou et al. [34] proposed a framework combining the autoencoder and the Gaussian process regression to address high-dimensional reliability analysis problems. Xiang et al. [35] proposed an active learning method combining deep neural

network and weighted sampling for structural reliability analysis. In recent years, with rapid advances in computing power, deep learning techniques have improved the state-of-the-art in image processing, natural language processing, audio processing, and many other appealing domains [36]. Recurrent neural network (RNN) [37,38] is a kind of neural network, which is able to handle a variable-length sequence input. GRU model [39,40] is a special kind of RNN that can solve its long-term dependence problem. Therefore, a GRU-based ensemble learning approach is developed for response analysis of structures with time-variant uncertainties in this paper. As shown in Fig. 1, multiple GRU networks are trained to learn the time-variant system response under fixed stochastic variables firstly. In the process of training GRU networks, an active learning strategy is proposed and applied to improve model accuracy and reduce the amount of training data needed. Furthermore, a set of augmented data can be collected based on multiple trained GRU networks. As a result, the mapping relationship between stochastic variables and structural responses can be built through the GP model. Finally, the global surrogate model of time-variant structural response is constructed by integrating the GRU network and the GP model.

The remainder of this paper is organized as follows. Section 2 starts with the theoretical background of finite element method for structure with uncertain parameters. Section 3 introduces the details of the proposed GRU-based ensemble learning framework. Section 4 presents two engineering examples to prove the accuracy and feasibility of the proposed method. Section 5 draws some conclusions about the paper.

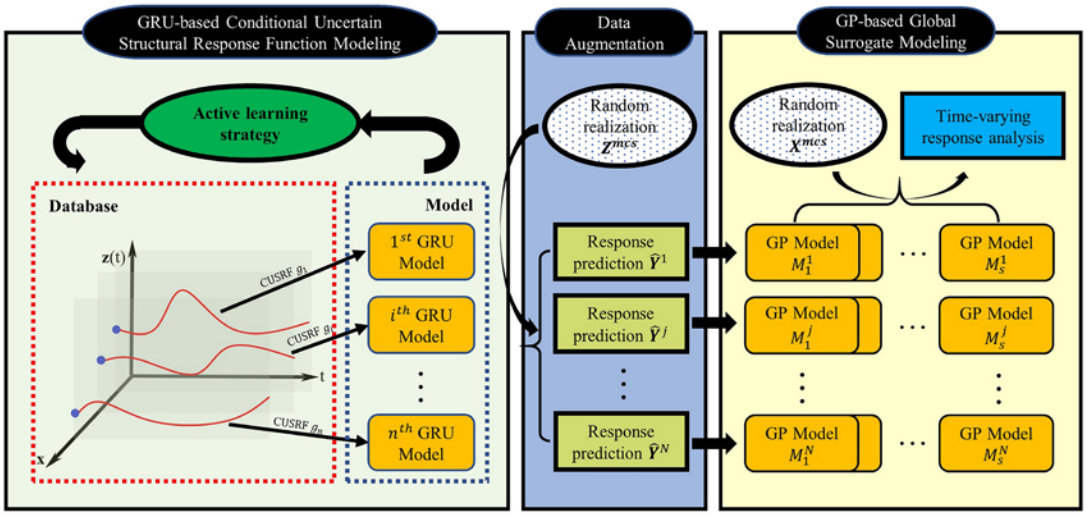

Fig.1 Sketch of the GRU-based ensemble learning (CUSRF: conditional uncertain structural response function)

2. Finite element equation with time-variant uncertainties

After discretization, the element displacement matrix $\boldsymbol{d}$ can be expressed as

$$\boldsymbol{d} = \boldsymbol{N}\boldsymbol{\delta}_e \tag{1}$$

where $\boldsymbol{N}$ represents the shape function matrix and $\boldsymbol{\delta}_e$ is a vector of the global displacement components at all nodal points, respectively. The strain within each element $\boldsymbol{\varepsilon}$ can be evaluated by establishing strain-displacement relationship

$$\boldsymbol{\varepsilon} = \boldsymbol{B}\boldsymbol{\delta}_e \tag{2}$$

where $\boldsymbol{B}$ stands for the strain matrix. According to the relationship between stress and strain, physical equations can be established

$$\boldsymbol{\sigma} = \boldsymbol{D}\boldsymbol{B}\boldsymbol{\delta}_e \tag{3}$$

where $\boldsymbol{D}$ is the elasticity matrix determined by the elastic constant of the element material. According to the principle of virtual displacements, the element stiffness equation can be expressed as

$$\boldsymbol{k}_e\boldsymbol{\delta}_e = \boldsymbol{F}_E^e \tag{4}$$

where $\boldsymbol{F}_E^e$ represents the element equivalent nodal forces vector caused by external effects. $\boldsymbol{k}_e$ is the element stiffness matrix, which can be obtained by

$$\boldsymbol{k}_e = \int_{\Omega_e} \boldsymbol{B}^T\boldsymbol{D}\boldsymbol{B}d\Omega \tag{5}$$

Eventually, by utilizing the direct stiffness method, each element stiffness matrix and element equivalent nodal forces vector are assembled to establish the nodal equilibrium equations for the entire system

$$\boldsymbol{K}\boldsymbol{U} = \boldsymbol{F} \tag{6}$$

where $\boldsymbol{K}$ is the global stiffness matrix; $\boldsymbol{F}$ is the global nodal force vector; $\boldsymbol{U}$ is the global nodal displacement vector. The nodal displacements can be obtained as

$$\boldsymbol{U} = \boldsymbol{K}^{-1}\boldsymbol{F} \tag{7}$$

It is noted that in this work, it is assumed that the time-variant parameters change slowly, so no additional inertial force is considered in the system. Therefore, considering the random variable and stochastic process mixed uncertain variables vector $C(\boldsymbol{x}, \boldsymbol{z}(t))$, the Eq. (7) can be rewritten as

$$\boldsymbol{U} = \boldsymbol{K}^{-1}(C)\boldsymbol{F}(C) = G(\boldsymbol{x}, \boldsymbol{z}(t), t) \tag{8}$$

3 GRU-based ensemble learning

3.1 GRU-based modeling

The RNN is an extension of a conventional feedforward neural network, which is able to handle time-series data by storing prior information with a feed-back loop. Unfortunately, it is difficult to train RNNs to capture long-term dependencies due to the

gradients tend to either vanish or explode. To reduce the negative impacts of this issue, all RNNs have the form of a chain of recurrent units such as LSTM unit or GRU. Compared with LSTM, GRU can achieve considerable results and is easier to train, which can greatly improve training efficiency. So we choose to use GRU in this paper. Similarly to the LSTM unit, two gated units are used in GRU, including a reset gate and update gate. Fig.2 shows the graphical depiction of GRU, which reflects that the core idea of GRU is to transmit the information flow by utilizing the cell state.

The effectiveness of the GRU network for handling time-dependent problems has been illustrated in countless research work. However, a lack of ability to take the time-independent random variables into account, which generally is the shortcoming of the GRU. Accordingly, instead of modeling the uncertain system $G(\boldsymbol{x}, \boldsymbol{z}(t), t)$ with mixed random variable and stochastic process directly, the concept of conditional uncertain structural response functions is introduced for GRU modeling. In the proposed approach, n samples of the random variables and the stochastic processes are generated using LHS. They can be expressed as $\boldsymbol{X} = [\boldsymbol{x}_1, \boldsymbol{x}_2, \dots, \boldsymbol{x}_n]$ and $\boldsymbol{Z} = [\boldsymbol{z}_1(t), \boldsymbol{z}_2(t), \dots, \boldsymbol{z}_n(t)]$ respectively. Compared with the simple random sampling of MCS, the LHS method produces a higher sample space coverage and can achieve higher sampling accuracy with a small sampling scale. For each sample $\boldsymbol{x}_i$ in $\mathbf{X}$, the conditional uncertain structural response function $g_i(\boldsymbol{z}_i(t), t)$ can be expressed as

$$g_i(\boldsymbol{z}_i(t), t) = G(\boldsymbol{x}_i, \boldsymbol{z}_i(t), t), i = 1,2, \dots, n \tag{9}$$

where $\boldsymbol{z}_i(t)$ represents the ith realizations of the stochastic processes $\boldsymbol{z}(\boldsymbol{t})$ and $\boldsymbol{x}_i$ denotes the ith realizations of the stochastic variables $\boldsymbol{x}$.

As shown in Eq. (9), each conditional uncertain structural response function is a simplified version of the original $G(\boldsymbol{x}, \boldsymbol{z}(t), t)$ with fixed random variables. For the ith conditional uncertain structural response function, substituting the inputs $\boldsymbol{x}_i$ and $\boldsymbol{z}_i(t)$ into Eq. (9), the time-variant structural responses $\boldsymbol{y}_i$ can be obtained. The GRU is a predictive model which can be trained to approximate the conditional uncertain structural response function. The input of the training data is expressed as a matrix

$$\begin{bmatrix} \boldsymbol{\eta}_1 \\ \boldsymbol{\eta}_2 \\ \vdots \\ \boldsymbol{\eta}_s \end{bmatrix} = \begin{bmatrix} \boldsymbol{z}_i(t_1) & t_1 \\ \boldsymbol{z}_i(t_2) & t_2 \\ \vdots & \vdots \\ \boldsymbol{z}_i(t_s) & t_s \end{bmatrix} \tag{10}$$

where $\boldsymbol{z}_i(t_j)$ represents the stochastic processes value at the j th time instant. Correspondingly, the training label for the GRU can be expressed as $\boldsymbol{y}_i = [y_i(t_1), y_i(t_2), \dots, y_i(t_s)]$, which is a vector with s elements.

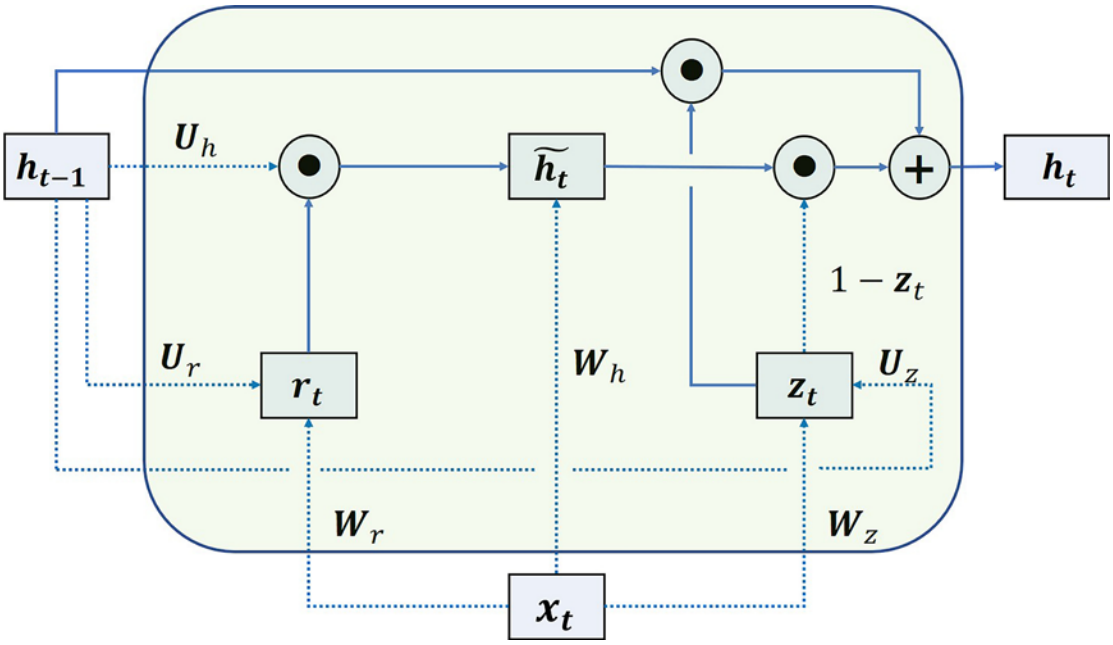

Fig.2 Recurrent units of GRU

First, in the recurrent units, the inputs at the particular time instant $\boldsymbol{\eta}_j$ and the previous cell hidden state $\boldsymbol{h}_{j-1}$ are provided to the reset gate, which is multiplied with

weight matrices and followed by bias. It can be expressed as

$$\boldsymbol{r}_j = \sigma\left(\boldsymbol{W}_r\boldsymbol{\eta}_j + \boldsymbol{U}_r\boldsymbol{h}_{j-1} + \boldsymbol{b}_r\right) \tag{11}$$

where $\sigma(\cdot)$ stands for the activation function. Usually, the logistic sigmoid function is adopted as the activation function of reset gate. $\boldsymbol{r}_j$ represents the reset gate output. $\boldsymbol{W}_r$, $\boldsymbol{U}_r$ and $\boldsymbol{b}_r$ represents the learned input weights, recurrent weights and bias, respectively. Similar to the reset gate, the update gate output $\boldsymbol{z}_j$ is computed as

$$\boldsymbol{z}_j = \sigma\left(\boldsymbol{W}_z\boldsymbol{\eta}_j + \boldsymbol{U}_z\boldsymbol{h}_{j-1} + \boldsymbol{b}_z\right) \tag{12}$$

Next, we need to decide what new information should be stored in the candidate hidden state. First, the reset gate determines how much information from the previous hidden state will be ignored. Then, a hyperbolic tangent activation function creates a candidate hidden state with current time instant input and the preserved information from the previous hidden state. The computation process can be expressed as

$$\widetilde{\boldsymbol{h}_j} = \tanh(\boldsymbol{W}_h\boldsymbol{\eta}_j + \boldsymbol{U}_h\left(\boldsymbol{r}_j \odot \boldsymbol{h}_{j-1}\right) + \boldsymbol{b}_h) \tag{13}$$

where $\boldsymbol{W}_h$, $\boldsymbol{U}_h$ and $\boldsymbol{b}_h$ are the input weights, recurrent weights and bias, respectively, $\widetilde{\boldsymbol{h}_j}$ represents the cell candidate hidden state and $\odot$ is an element-wise multiplication.

Then, all the outputs of Eqs. (12) and (13) are utilized to update the current hidden state, written as

$$\boldsymbol{h}_j = \left(1 - \boldsymbol{z}_j\right) \odot \boldsymbol{h}_{j-1} + \boldsymbol{z}_j \odot \widetilde{\boldsymbol{h}_j} \tag{14}$$

In which, the first term represents selective forgetting of the previous hidden state, and the second term represents how much information from the new candidate hidden state should be retained in the current hidden layer. In addition, the weights of forgetting the previous hidden state and remembering the candidate hidden state are interrelated

to maintain a constant state.

In this study, the output $\boldsymbol{h}_j$ is directly linked to the fully connected layer and then the fully connected hidden layer is connected to the regression output layer, which is related with training label. The identical unit is repeated at each time step. According to the GRU structure introduced above, the gradients of weights and biases term need be calculated accordingly with the purpose of minimizing the loss function. Given the training data, in order to learn the weight matrices and biases of the GRU, we can choose optimization algorithms such as stochastic gradient descent with momentum (SGDM), root mean square propagation (RMSProp), and Adam to update the model parameters. In this work, the root mean square error (RMSE) is adopted as the loss function. The Adam is utilized as the optimization algorithm. n GRU models are respectively constructed to capture the relationship between the stochastic processes and time-variant responses of the conditional uncertain structural response functions.

3.2 Active learning strategy

The accuracy of the surrogate model is a challenge in the uncertain analysis. Surrogate model approaches based on deep learning are data-hungry as we all know. The more training data, the better the training results will be. Nevertheless, preparing considerable training samples is time-consuming and impractical in many applications. Active learning can help to ensure the model accuracy and reduce the amount of training data. On the other hand, in many engineering practices, uncertain variables are generally subject to a certain probability distribution. It needs relatively sufficient sample data to accurately propagate the statistical characteristics of the uncertainties

when using surrogate model. Otherwise the estimated probability characteristics will deviate from the true value, the uncertain system response will be unreliable. Then optimization based on the unreliable uncertain system response may fail to achieve the expected effect. Iteratively updating the surrogate model through active learning strategy can alleviate this situation to a certain extent. With comprehensive consideration, an active learning strategy is proposed here to reduce the amount of training data in the process of training GRU model while ensuring its accuracy.

Sample selection is a key component in the active learning. The strategy of sample selection is determined by query function F_q, which is expressed as:

$$F_q = \frac{\alpha}{d}\sum_{p=1}^{d}\left(\frac{2}{1+e^{-\left|\frac{\mu_p - x_p}{\sigma_p}\right|}} - 1\right) + \beta\left|\frac{y-\hat{y}}{y}\right| = \alpha F_{q1} + \beta F_{q2} \qquad (15)$$

where α and β are weighting coefficients which range from 0 to 1. They denote the importance of different parts in the query function. The query function consists of two parts, which can be interpreted from the perspective of input and output. The first part F_{q1} uncovers the correlation between test set input and training set input, which is inspired by the t-test [41]. In addition, the difference between these two data sets is scaled to [0,1] using the variant of sigmoid function. d represents the dimension of input variable, μ_p and σ_p represent the mean value and standard deviation in the current training set at the certain dimension p. The second part F_{q2} measures the deviation of test set between the predicted value and actual output. For n samples of the stochastic processes generated by LHS, we choose one sample of stochastic processes as the initial training set, and regard the remaining $n-1$ samples as the test set. When $\alpha + \beta = 1$, the query function is normalized to [0,1]. Next, the threshold ϵ_{th} decide if test set

sample can be added to previous training data for the next iteration of training. The detail value of α, β and ϵ_{th} needs to be determined based on specific occasion.

3.3 Gaussian Process-based global surrogate modeling

The GRUs have a high prediction accuracy for the conditional uncertain structural response functions when n random variables are fixed. Nevertheless, these GRUs still endure a drawback that they lack the capability of modeling the global uncertain structural response function with the time-independent random variables. To overcome this difficulty, Gaussian process regression is used to map the relationship between random variables and time-variant system responses at a specific time. Then, a global surrogate model can be constructed by integrating multiple Gaussian process regressions with GRUs to predict the time-variant system response given any random realizations of time-independent variables $\boldsymbol{x}'$ and stochastic processes $\boldsymbol{z}'(t)$.

In the data preparation process, the random realization $\boldsymbol{z}'(t)$ is provided to the constructed n GRUs for estimating the time-variant responses of the corresponding conditional uncertain structural response functions. Therefore, the response predictions of all the GRUs can be collected as

$$\widehat{\boldsymbol{Y}}' = [\widehat{\boldsymbol{y}}_1', \widehat{\boldsymbol{y}}_2', \dots, \widehat{\boldsymbol{y}}_n']^T = \begin{bmatrix} \hat{y}_1'(t_1) & \cdots & \hat{y}_1'(t_s) \\ \vdots & \ddots & \vdots \\ \hat{y}_n'(t_1) & \cdots & \hat{y}_n'(t_s) \end{bmatrix} \tag{16}$$

where the time-variant responses $\widehat{\boldsymbol{y}}_i'$ are the GRU predictions when giving the $\boldsymbol{z}'(t)$ related to the ith conditional uncertain structural response function g_i, which can be expressed as

$$\widehat{\boldsymbol{y}}_i' \approx g_i(\boldsymbol{z}'(t), t), t = t_1, \dots, t_s \tag{17}$$

Though the responses are not obtained by directly calculating the actual conditional uncertain structural response functions, the prediction accuracy is assured due to the benefits of GRU. As a result, the response predictions $\widehat{\boldsymbol{Y}}'$ are referred to as augmented data in this paper. To ensure the capability of estimating the time-variant responses with input $\boldsymbol{x}'$, GP models are constructed at each time instant based on the augmented data. Compared with the general regression method, Gaussian process regression is a less parametric tool. Given a specified time instant t_k, a GP model is built based on the training labels $\widehat{\boldsymbol{y}}'(t_k)$ extracted from the augmented data, which is expressed as

$$\widehat{\boldsymbol{y}}'(t_k) = [\hat{y}_1'(t_k), \hat{y}_2'(t_k), \dots, \hat{y}_n'(t_k)]^T \tag{18}$$

And the training inputs are the random samples $\boldsymbol{X} = [\boldsymbol{x}_1, \boldsymbol{x}_2, \dots, \boldsymbol{x}_n]$. Gaussian process regression is based on the assumption that the functional relationship between the input and output data can be modeled by a sample path of a Gaussian process. Therefore, the relationship between input and the training label is defined as

$$\hat{y}_i'(t_k) = g(\boldsymbol{x}_i) + \epsilon \tag{19}$$

where ϵ is the Gaussian noise with zero mean and variance ${\sigma_n}^2$. $g(\boldsymbol{x}_i)$ is the learning function. From the function-space view, a Gaussian process with a non-zero mean function can be written as

$$g(\boldsymbol{x}) \sim GP\left(\boldsymbol{h}(\boldsymbol{x})\boldsymbol{\beta}, K(\boldsymbol{x}^a, \boldsymbol{x}^b)\right) \tag{20}$$

where $\boldsymbol{h}(\boldsymbol{x})\boldsymbol{\beta}$ represents mean function and $K(\boldsymbol{x}^a, \boldsymbol{x}^b)$ represents covariance function. The term $\boldsymbol{h}(\boldsymbol{x})$ are a set of predefined basis function. Linear basis function is used in this research. $\boldsymbol{\beta}$ is a vector of basis function coefficients. The covariance function is

computed by

$$K(\boldsymbol{x}^a, \boldsymbol{x}^b) = {\sigma_s}^2 R(\boldsymbol{x}^a, \boldsymbol{x}^b, \boldsymbol{\theta}) = {\sigma_s}^2 \exp\left[\sum_{p=1}^{d} \theta_p \left|\boldsymbol{x}_p^a - \boldsymbol{x}_p^{\mathrm{b}}\right|^2\right] \tag{21}$$

where ${\sigma_s}^2$ is the signal variance and the auto-correlation $R(\cdot)$ defines the nearness or similarity between every pair of sample points $(\boldsymbol{x}^a, \boldsymbol{x}^b)$ in the input space. The hyperparameters $\boldsymbol{\theta}$ denote a set of unknowns which characterize the decay of auto-correlation with distance. In more detail, θ_p is the correlation length of each dimension $p \in [1, d]$ of the input $\boldsymbol{x}$. The GP model M_k' are described as

$$M_k'(\boldsymbol{x}) | \boldsymbol{z}'(t_k), t_k \sim GP(\boldsymbol{h}(\boldsymbol{x})\boldsymbol{\beta}, K(\boldsymbol{x}^a, \boldsymbol{x}^b) + {\sigma_n}^2 \boldsymbol{I}) \tag{22}$$

where $\boldsymbol{I}$ is the identity matrix. For a prediction point $\boldsymbol{x}'$, the joint Gaussian distribution of the observed target values and the predicted values is given by

$$\begin{bmatrix} \widehat{\boldsymbol{y}}'(t_k) \\ g(\boldsymbol{x}') \end{bmatrix} \sim GP\left(\begin{bmatrix} \boldsymbol{h}(\boldsymbol{X})\boldsymbol{\beta} \\ \boldsymbol{h}(\boldsymbol{x}')\boldsymbol{\beta} \end{bmatrix}, \begin{bmatrix} K(\boldsymbol{X}, \boldsymbol{X}) + {\sigma_n}^2 \boldsymbol{I} & K(\boldsymbol{X}, \boldsymbol{x}') \\ K(\boldsymbol{x}', \boldsymbol{X}) & K(\boldsymbol{x}', \boldsymbol{x}') \end{bmatrix}\right) \tag{23}$$

The predicted mean value $m(\boldsymbol{x}')$ is given as

$$m(\boldsymbol{x}') = \boldsymbol{h}(\boldsymbol{x}^*)\boldsymbol{\beta} + {K'}^T (K(\boldsymbol{X}, \boldsymbol{X}) + {\sigma_n}^2 \boldsymbol{I})^{-1} (\widehat{\boldsymbol{y}}'(t_k) - \boldsymbol{h}(\boldsymbol{X})\boldsymbol{\beta}) \tag{24}$$

and the variance $v(\boldsymbol{x}')$ is

$$v(\boldsymbol{x}') = K(\boldsymbol{x}', \boldsymbol{x}') - {K'}^T (K(\boldsymbol{X}, \boldsymbol{X}) + {\sigma_n}^2 \boldsymbol{I})^{-1} K' + {\sigma_n}^2 \boldsymbol{I} \tag{25}$$

where $K' = K(\boldsymbol{x}, \boldsymbol{x}')$ present the correlation vector between $\boldsymbol{x}'$ and training points $\boldsymbol{X}$. The unknown hyperparameters $\boldsymbol{\beta}$, ${\sigma_n}^2$ and $\boldsymbol{\theta}$ fully characterize the GP model, which can be obtained by maximizing marginal log-likelihood function using standard optimization algorithms.

In this work, the resultant predicted mean value $m(\boldsymbol{x}')$ is adopted as the response estimation of $G(\boldsymbol{x}', \boldsymbol{z}'(t_k), t_k)$. Given a specific stochastic process, a set of GP models can be constructed based on the augmented data set which includes the training inputs

$\boldsymbol{X} = [\boldsymbol{x}_1, \boldsymbol{x}_2, \dots, \boldsymbol{x}_n]$ and the training labels $\widehat{\boldsymbol{y}}'(t_k)\ k = 1, \dots, s$. As a consequence, the time-variant responses of $G(\boldsymbol{x}', \boldsymbol{z}'(t), t)$ can be predicted by s GP models. According to the probability statistics characteristics of the random variables and the stochastic processes, N random realizations are generated respectively as MCS samples, which are $\boldsymbol{X}^{mcs} = [\boldsymbol{x}_1{}^m, \boldsymbol{x}_2{}^m, \dots, \boldsymbol{x}_N{}^m]$ and $\boldsymbol{Z}^{mcs}(t) = [\boldsymbol{z}_1{}^m(t), \boldsymbol{z}_2{}^m(t), \dots, \boldsymbol{z}_N{}^m(t)]$. For all the stochastic processes samples in MCS $\boldsymbol{Z}^{mcs}(t)$, a total number of $N \times s$ GP models can be constructed. By combining the multiple GRUs and the GP models, the global surrogate model of the time-variant response can be obtained. Given any realization of the random variables and stochastic processes, the proposed ensemble learning framework can provide response predictions in a global sense.

3.4 Response analysis of time-variant uncertain structures

The main steps of proposed ensemble learning method for response analysis of time-variant structural system under the mixed uncertainty model with random variables and stochastic processes can be summarized as follows

Step 1: Produce the sampling data for training multiple GRU models. LHS is employed to generate n samples of random variables $\boldsymbol{X} = [\boldsymbol{x}_1, \boldsymbol{x}_2, \dots, \boldsymbol{x}_n]$ and n realizations of the stochastic processes $\boldsymbol{Z} = [\boldsymbol{z}_1(t), \boldsymbol{z}_2(t), \dots, \boldsymbol{z}_n(t)]$.

Step 2: Evaluate actual responses of time-variant structural system with the samples obtained in last step.

Step 3: Construct multiple GRUs for conditional uncertain structural response function $g_i(\boldsymbol{z}_i(t), t)$.

Step 4: Determine whether active learning is required according to RMSE of test sets.

Use the query function to update database if necessary. And then, repeat 3-4 until the RMSE of test sets is satisfied.

Step 5: Collect response predictions for $\boldsymbol{Z}^{mcs}$ using each GRU.

Step 6: Obtain training outputs $\hat{\boldsymbol{y}}^j(t_k)$ as the augmented data and build $N \times s$ GP models for global response analysis of time-variant structural system.

Step 7: Obtain all the time-variant response predictions for $\boldsymbol{X}^{mcs}$ and calculate the mean and standard deviation of system response.

The flowchart of the proposed ensemble learning method is shown in Fig. 3.

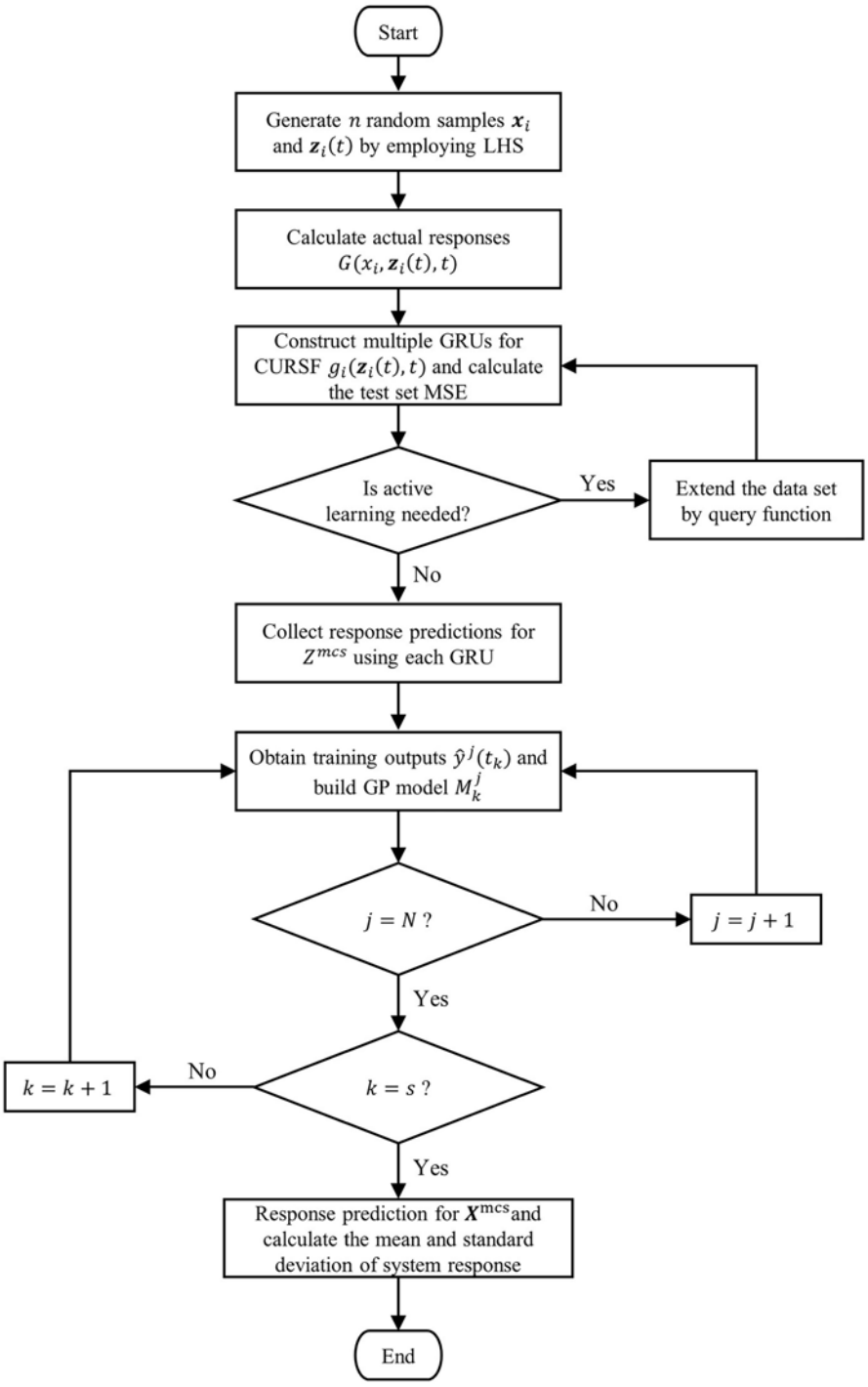

Fig.3 Flowchart of the proposed ensemble learning framework

4 Numerical example and analysis

In this section, two engineering examples are considered to verify the effectiveness of the proposed approach. All the simulation are carried out by using MATLAB R2020a

on a 2.90GHz Intel(R) Core(TM) CPU i5-10400.

4.1 Plane truss structure

Fig. 4 depicts the geometry of a plane truss structure, which is composed of six nodes and nine bars. The plane truss is fixed at point A, hinged at point B and subjected to a concentrated stochastic load F_L at point E.

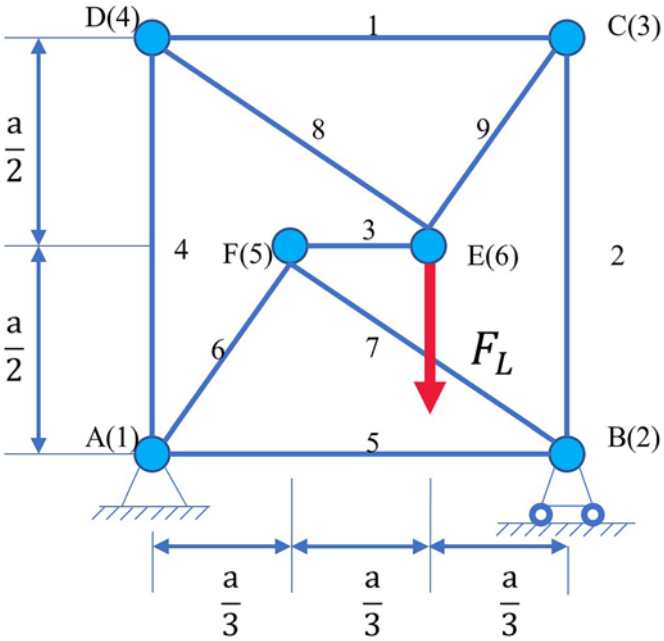

Fig.4 Geometry of the 9-bar truss structure

In practical engineering, the uncertainties inevitably exist in the truss system. Due to the manufacturing error, the cross-sectional area of the connecting rod A $(10^{-4}\mathrm{m}^2)$ and the length of the longest bar $a(m)$ are both treated as a random variable following a normal distribution, where $A \sim N(1, 0.1^2)$ and $a \sim N(1, 0.1^2)$. Considering the unevenness of the material, the Young's modulus of material E (GPa) is also modeled as Gaussian variable, where $E \sim N(200, 20^2)$. Furthermore, since the influence of environmental factors such as humidity and temperature, the material density $\rho(t)$ (g/cm^3) and stochastic load $F_L(t)$ (kN) are assumed to follow a non-stationary

Gaussian process. Taking the stochastic load as an example, it is characterized by its mean function $\mu_{F_L}(t)$, standard deviation function $\sigma_{F_L}(t)$, and autocorrelation function $p_{F_L}(t)$, which can be expressed as

$$\mu_{F_L}(t) = e^{-0.01t}\sin\left(0.05\pi t + \frac{\pi}{4}\right) + m_F \tag{25}$$

$$\sigma_{F_L}(t) = e^{-0.01t}\sin\left(0.05\pi t + \frac{\pi}{4}\right) + s_F \tag{26}$$

$$p_{F_L}(t_1, t_2) = \exp\left(-\frac{0.0001(t_2 - t_1)^2}{\lambda_F}\right) \tag{27}$$

where m_{F_L}, s_{F_L} and λ_{F_L} are assigned to be -1, 0.08, 0.005, respectively. Similar to stochastic load, the variables m_ρ, s_ρ and λ_ρ are assigned to be 2, 0.1, 0.01, respectively. In this example, the considered time period is $100\ s$, which is discretized into 100 time nodes. The displacement response at point E is calculated.

Firstly, to prepare the training data for the GRU models, eight samples of random variables $\boldsymbol{x}$ and stochastic processes $\boldsymbol{z}(t)$ are generated by employing LHS. Then, the corresponding time-variant responses are computed based on finite element analysis. Given the training data sets, eight GRU models are constructed respectively. Fig. 5(a)-(b) depicts eight random realizations of the stochastic processes, which are utilized as the test set input corresponding to each GRU model. Furthermore, the resultant time-variant responses are shown in Fig. 5(c). In the GRU model, the layers number of the GRU is set to two. Each layer has 50 neurons. The number of layers and neurons is decided by manually tuning here. All the GRU models are trained by using Adam optimizer to minimize the RMSE with 200 epochs.

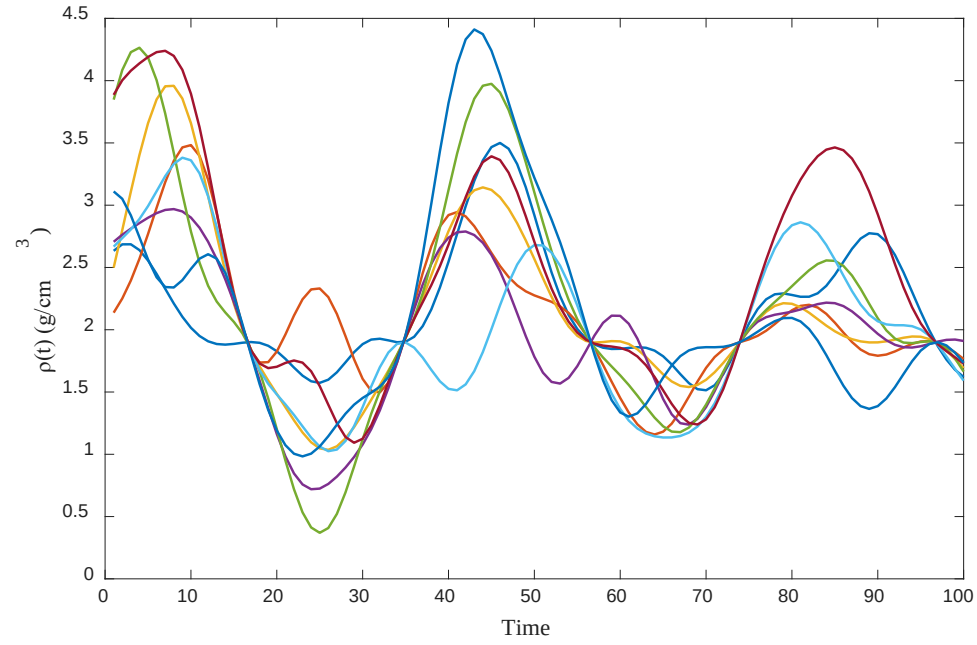
4.5
4
3.5
3
2.5
2
1.5
1
0.5
0
ρ(t) (g/cm 3)
0
10
20
30
40
50
60
70
80
90
100
Time

(a) $\rho(t)$

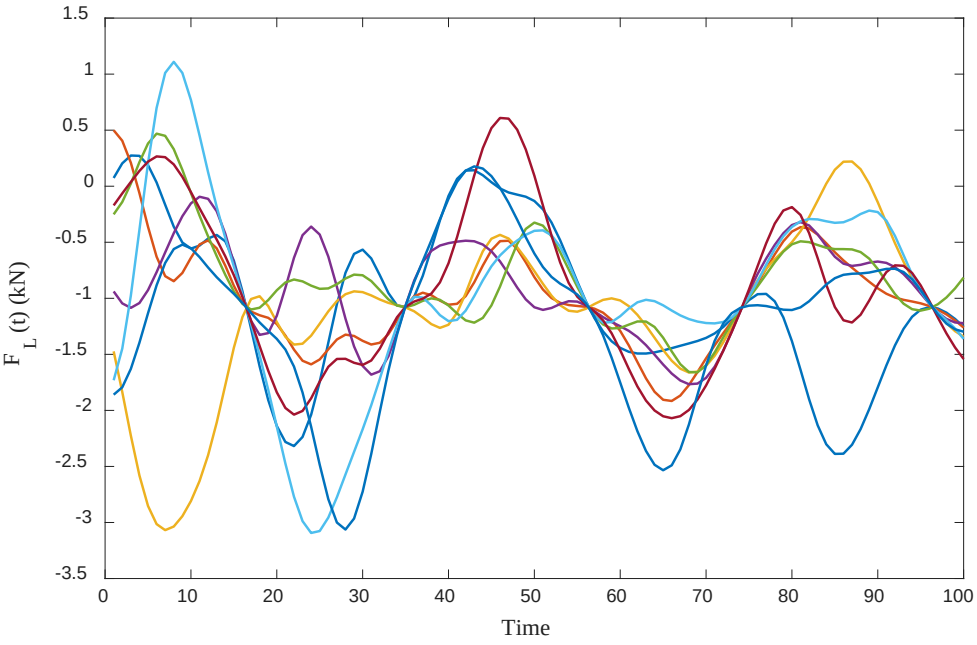
1.5
1
0.5
0
-0.5
-1
-1.5
-2
-2.5
-3
-3.5
F L (t) (kN)
0
10
20
30
40
50
60
70
80
90
100
Time

(b) $F_L(t)$

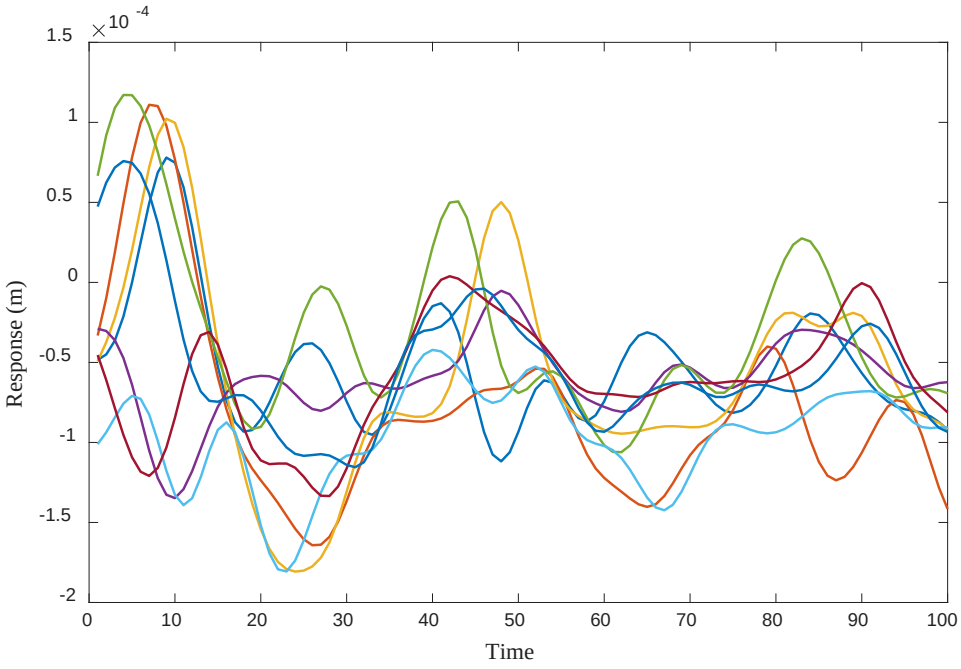

(c) The displacement of point E

Fig. 5 Eight realizations of stochastic processes and resultant time-variant responses

In order to train GRU model better, an active learning strategy is adopted according to the RMSE of the test set. Nine sets of weighting and threshold are chose. Fig. 6 shows the comparison of the effect of active learning and random sampling under different parameter selection. The results demonstrate that active learning can achieve better results than random sampling no matter what the parameters are selected. It can be seen that the RMSE curve fluctuates greatly during iterations. This phenomenon is justified because that the test set is different each time. Therefore, the training accuracy of GRU may not be ideal on individual extreme test sets. But the RMSE presents a decreasing trend as the number of iterations increases. In addition, the effect of active learning becomes worse as the threshold ϵ_{th} increase. This is because the more severe the conditions, the less data will be added to the next round of training, so the training results may not be ideal. This is a common trade-off problem in engineering practice,

and we need to choose the threshold value according to actual needs. In this case, $\alpha = 0.5$, $\beta = 0.5$ and the threshold ϵ_{th} is set to 0.2. Fig. 7 depicts the comparison of the actual and predicted time-variant responses to demonstrate that the GRU is capable of accurately capturing the relationship between the stochastic processes and the time-variant responses. Fig. 7(a) shows the response comparison of the first GRU on the test set implemented randomly and Fig. 7(b) shows the response comparison of the eighth GRU on the test set implemented randomly. The results demonstrate that the GRU models have been well trained and thus are capable of accurately predicting the time-variant responses of the conditional uncertain structure with respect to any realizations of the stochastic processes.

For a single GRU network, we recorded the average training time $T_{train} = 4.25s$. Considering the proposed active learning strategy, the final computational time required for iteratively training a GRU network can be expressed as $T_{final} = T_{train} \times Ite$. Ite represents the number of iterations. To avoid too many iterations, the maximum number of iterations Ite_{max} is adopted and set as 15 according to the experimental results, which is shown in Fig. 6(h). It is noted that all the GRU models are trained using the NVIDIA GeForce GTX 1650 GPU. Because the call time of a GRU model is extremely short. Therefore, the entire process of using the GRU model, including the training process, has a very small computational cost compared with MCS, especially when a time-consuming finite element analysis needs to be implemented to obtain the structural response.

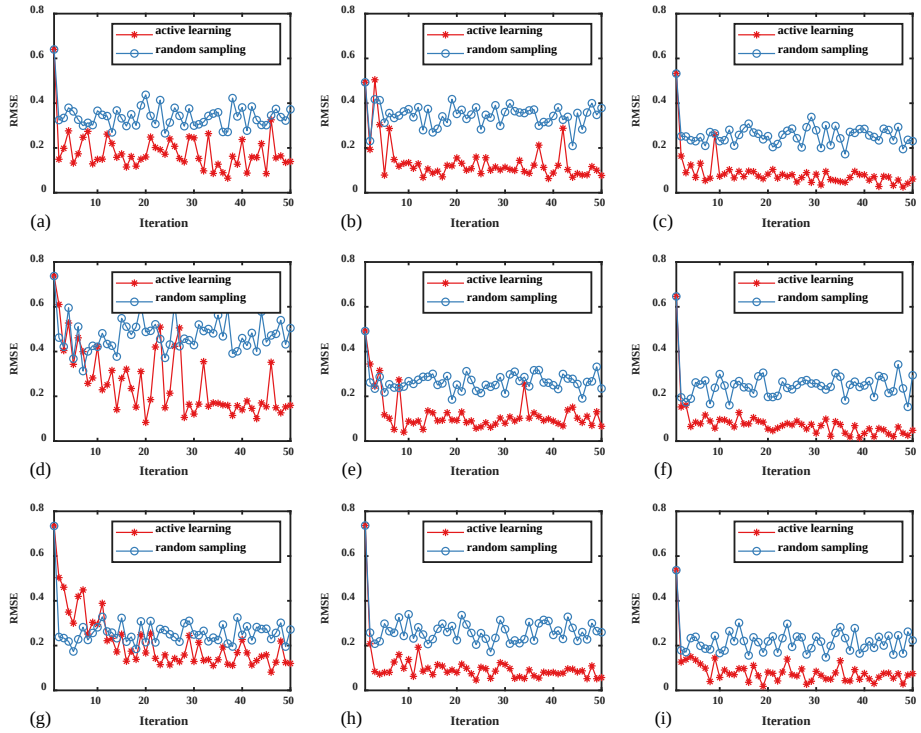

Fig. 6 Comparisons the RMSE of the test set between active learning and random sampling: (a) $\alpha = 0.2$, $\beta = 0.8$, $\epsilon_{th} = 0.8$, (b) $\alpha = 0.5$, $\beta = 0.5$, $\epsilon_{th} = 0.8$, (c) $\alpha = 0.8$, $\beta = 0.2$, $\epsilon_{th} = 0.8$, (d) $\alpha = 0.2$, $\beta = 0.8$, $\epsilon_{th} = 0.5$, (e) $\alpha = 0.5$, $\beta = 0.5$, $\epsilon_{th} = 0.5$, (f) $\alpha = 0.8$, $\beta = 0.2$, $\epsilon_{th} = 0.8$, (g) $\alpha = 0.2$, $\beta = 0.8$, $\epsilon_{th} = 0.2$, (h) $\alpha = 0.5$, $\beta = 0.5$, $\epsilon_{th} = 0.2$, (i) $\alpha = 0.8$, $\beta = 0.2$, $\epsilon_{th} = 0.2$.

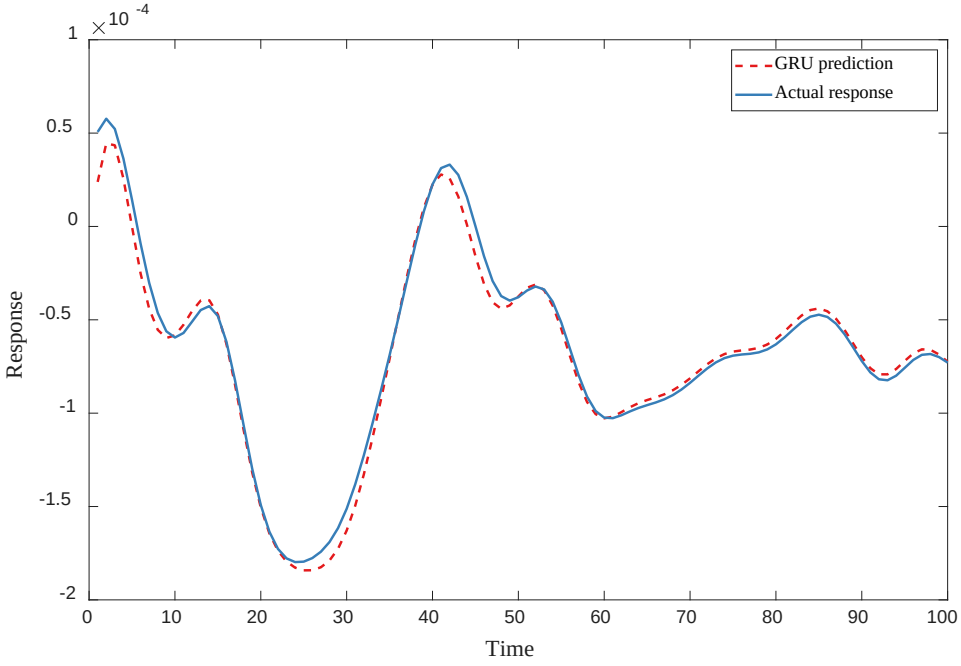

(a)

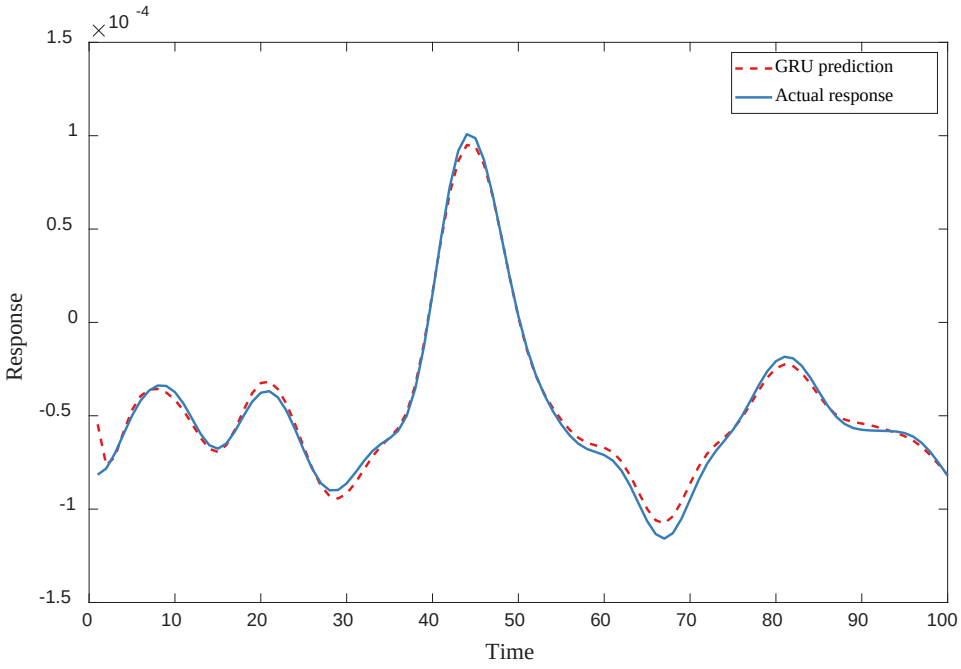

(b)

Fig. 7 Comparisons between actual responses and estimations by GRU models

For each GRU model, 10000 MCS samples of stochastic processes are generated for predicting the time-variant structural responses of the conditional uncertain structure response functions, which is the augmented data. After obtaining the augmented data, GP models at a specific time and a specific random process can be constructed. Then, the response of the time-variant uncertain structure can be calculated based on the GP models and 10000 MCS samples of the random variables. To demonstrate the accuracy of time-variant response predictions using GP models, Fig. 8 shows the comparison of the accurate and predicted time-variant responses with respect to the $50th$ and $100\,th$ MCS samples, respectively. The results demonstrate that the constructed GP models can effectively handle the time-independent variables, and they can provide accurate response predictions for the whole time-series data.

To validate the accuracy of response analysis, the actual time-variant system

responses with respect to the 10000 MCS samples of stochastic process and random variable are calculated directly, and their resultant mean and standard deviation are computed as the reference solution. For comparison, the response surface method (RSM) is adopted here for approximating the time-variant response analysis. The comparison between the response obtained by using the proposed approach and the RSM is shown in Fig. 9. It can be seen that the mean value obtained by the proposed method is almost the same as the reference solutions, and the deviation of the standard deviation obtained by the proposed method from the reference solutions is very small. This indicates that the proposed method can predict the uncertain system response with high precision under the mixed model of random variables and random processes. It should be noted that the reference solutions here are obtained by the direct MCS method, which includes $10000 \times 10000 = 10^8$ calls of the uncertain structural response function. Whereas, the proposed method only needs 8 calls of the uncertain structural response function to obtain the global surrogate model. The following calculations are based on the surrogate model to calculate the mean and standard variance, which approaches to the reference solutions very well. Furthermore, by utilizing the same number calls of the uncertain structural response function, 100 response surface surrogate models in total are constructed at different time instants. The average relative error rate throughout the time period is calculated here to quantify the accuracy. The average relative error rate of the mean of displacement at node E calculated by the proposed approach and RSM are 4.39% and 10.72%, respectively. As for the standard deviation of displacement at node E, the average relative error rate calculated by the

proposed approach and RSM are 3.85% and 16.92%, respectively. In comparison, with the same amount calls of the uncertain structural response function, the computational accuracy obtained by the proposed method is much better.

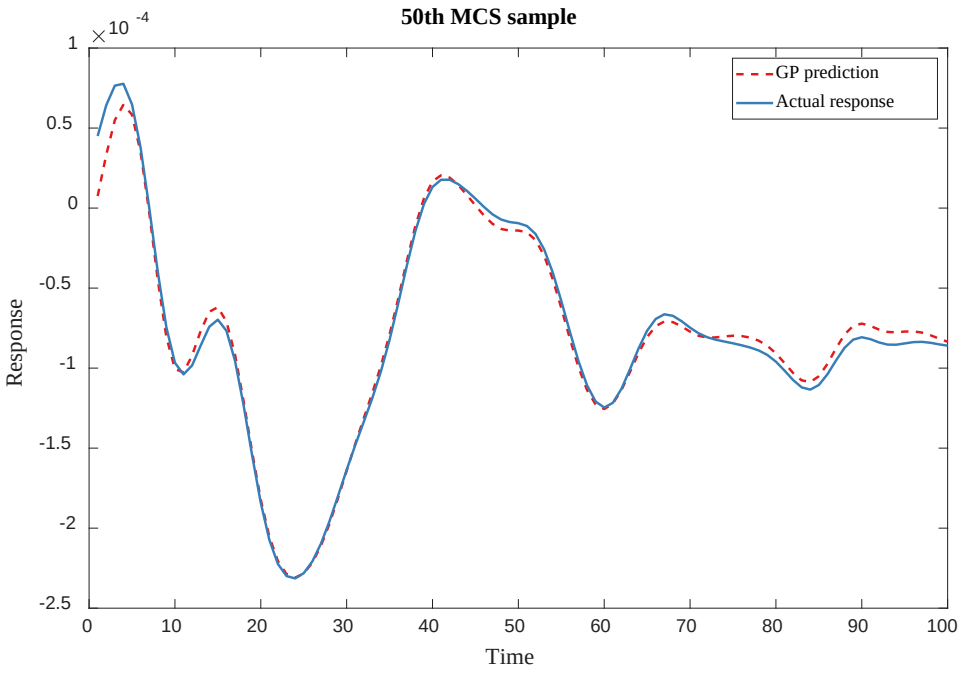

(a)

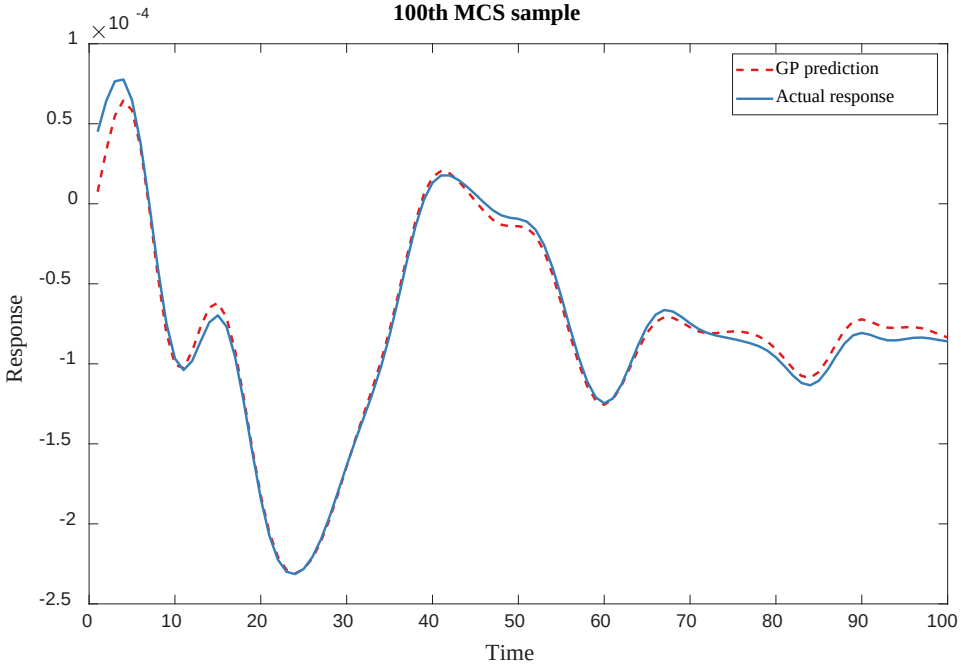

(b)

Fig. 8 Comparisons between the actual and estimated time-variant responses

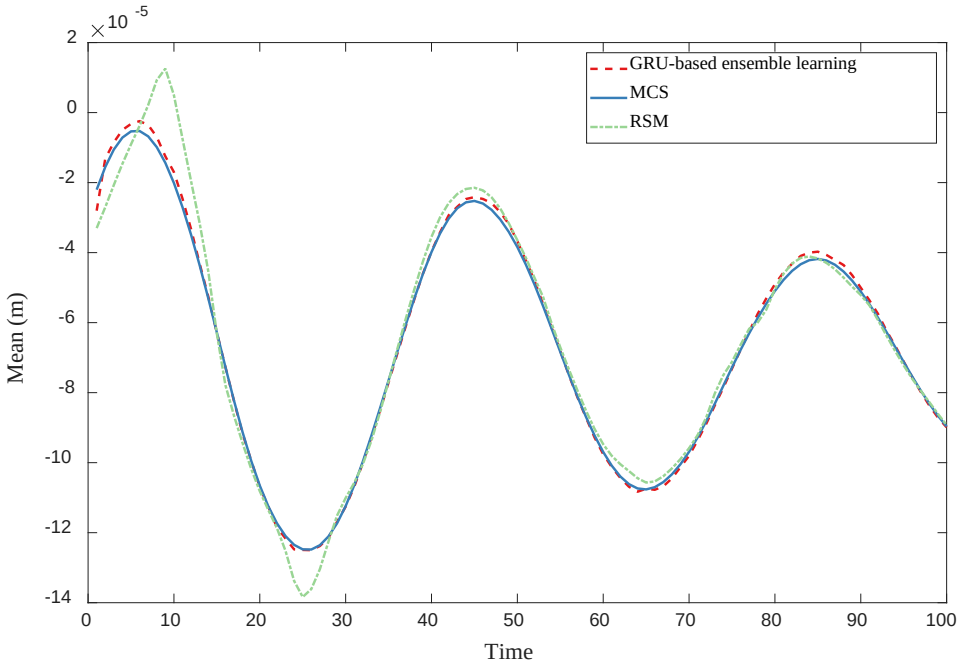

（a）

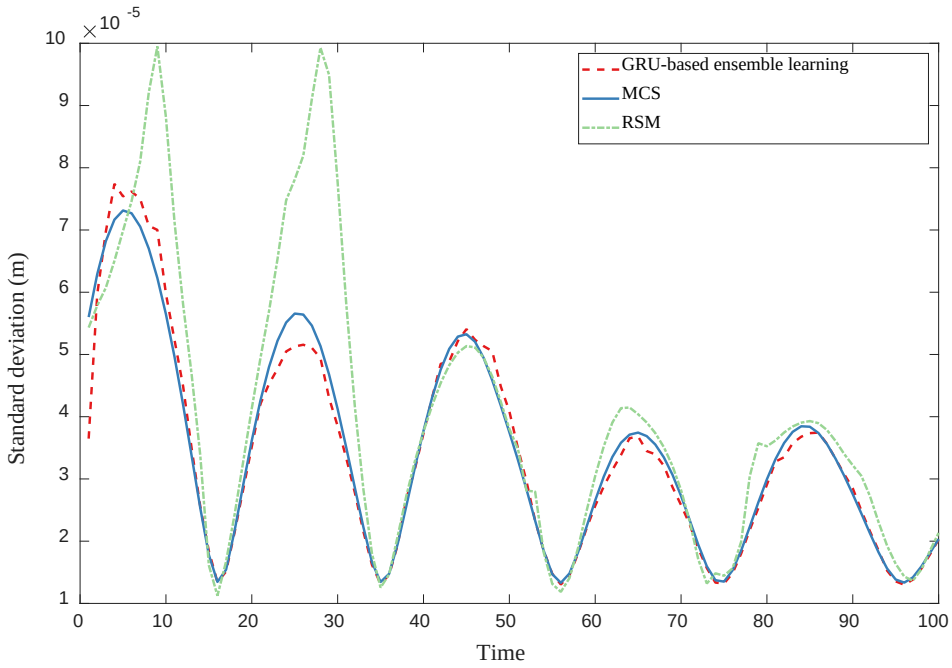

(b)

Fig. 9 The mean and standard deviation of displacement at node E: (a) mean (b) standard deviation

4.2 Continuum shell structure

In this section, a continuum shell structure under mixed uncertainty model with random variable and stochastic process is considered to investigate the effectiveness of proposed method. The shell structure is shown in Fig. 10. It is divided into the quadrilateral elements. The number of elements is 16 and the number of nodes is 25. The shell structure is excited by a stochastic load $F(t)\ kN$ along the z axis at the center. All of the edges are fixed.

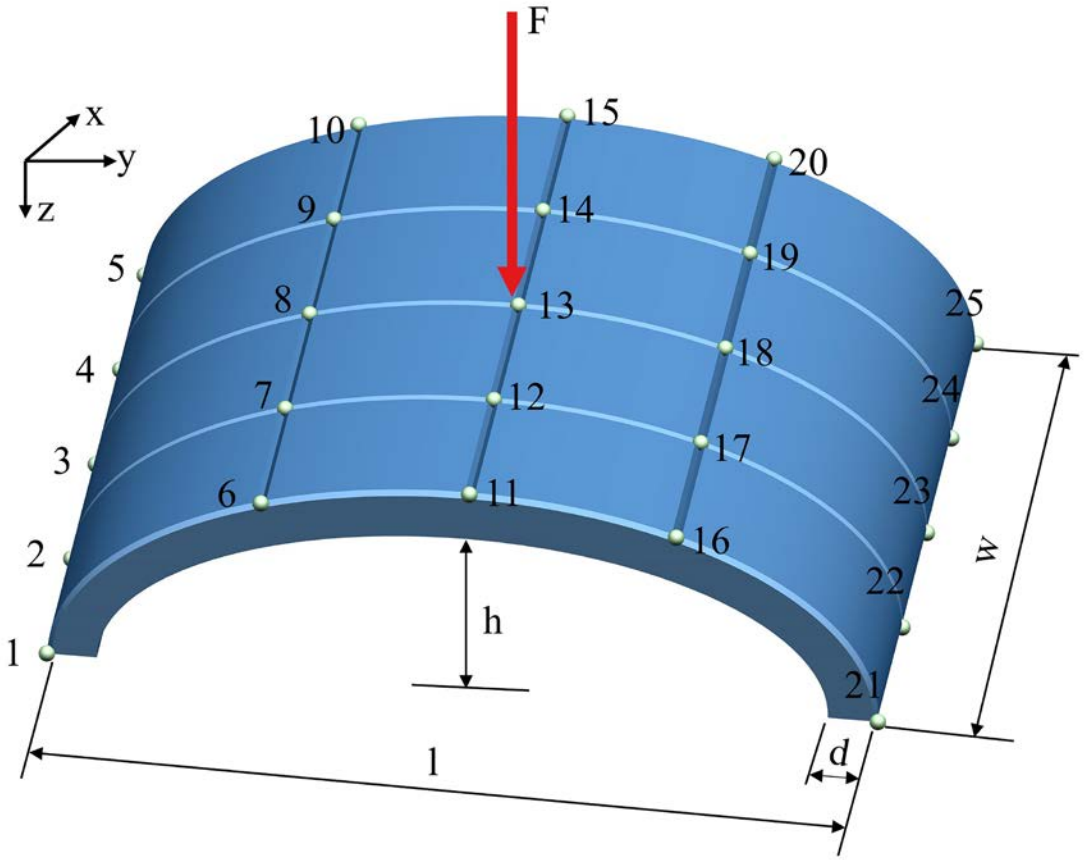

Fig.10 The shell structure

Considering manufacturing and assembly errors, The length l (m), width w (m) height h (m) and thickness d (m) of cylindrical shell structure are assumed as random variables that follow normal distributions, where $l \backsim N(50, 5^2)$, $w \backsim N(50, 5^2)$, $h \backsim$

$N(25, 2.5^2)$ and $d \backsim N(0.25, 0.025^2)$. Considering the uncertainty in material properties and the unpredictability of environmental load, the Young's modulus $E(t)$ (GPa), the Poisson's ratio $v(t)$ and the stochastic load $F(t)$ are treated as non-stationary Gaussian process. The detail probabilistic information of each non-stationary Gaussian process variables are listed in Table 1. In this study, the time interval $[0, 100]$ is discretized into 100 time nodes. 5000 MCS samples are generated for the response analysis of time-variant uncertain structures after building the GRU-based ensemble learning framework. The displacement response at the thirteenth node is calculated.

Table 1 The probabilistic information of non-stationary Gaussian process variables

Variable	Mean function	Standard deviation function	Autocorrelation function
$F(t)$ (kN)	$e^{-0.01t}\sin\left(0.05\pi t+\frac{\pi}{4}\right)+5$	$e^{-0.01t}\sin\left(0.05\pi t+\frac{\pi}{4}\right)+0.15$	$exp(-0.01(t_2-t_1)^2)$
$v(t)$	$e^{-0.01t-2}+0.25$	$2e^{-0.01t-20}+0.005$	$exp(-\frac{0.1(t_2-t_1)^2}{5})$
$E(t)$ (GPa)	$t+206$	$0.05t+5$	$exp(-\frac{0.01(t_2-t_1)^2}{3})$

The proposed approach is employed to solve the displacement response problem of shell structure, where forty training data sets are utilized for training the GRU models. In the GRU model, the layers number of the GRU is set to two. Each layer has 40 neurons. The GRU models are trained with a maximum epochs 1000. To validate the effectiveness of the active learning strategy, the comparison of the effect of active learning and random sampling when $\alpha = 0.5$, $\beta = 0.5$ and $\epsilon_{th} = 0.2$ is shown in Fig. 11. The results demonstrate that the use of active learning can achieve high training accuracy with a relatively small amount of data. At the same time, for large-scale engineering problems, less data will reduce training time. The iterative update process

also makes the proposed method robust. Fig. 12 shows the convergence of the RMSE loss function for the first GRU. Similar convergence curves can be observed for other GRU models. To validate the accuracy and effectiveness of the GRU, the comparison of the actual responses and the predicted responses by the first GRU model on the test set implemented randomly is shown in Fig. 13. The results demonstrate that GRU models can make accurate response predictions for the conditional uncertain structure response functions with respect to any random realizations of the stochastic processes. Therefore, although the augmented data are not collected directly from the uncertain structural functions, the accuracy is guaranteed due to the good training effect of the GRU model.

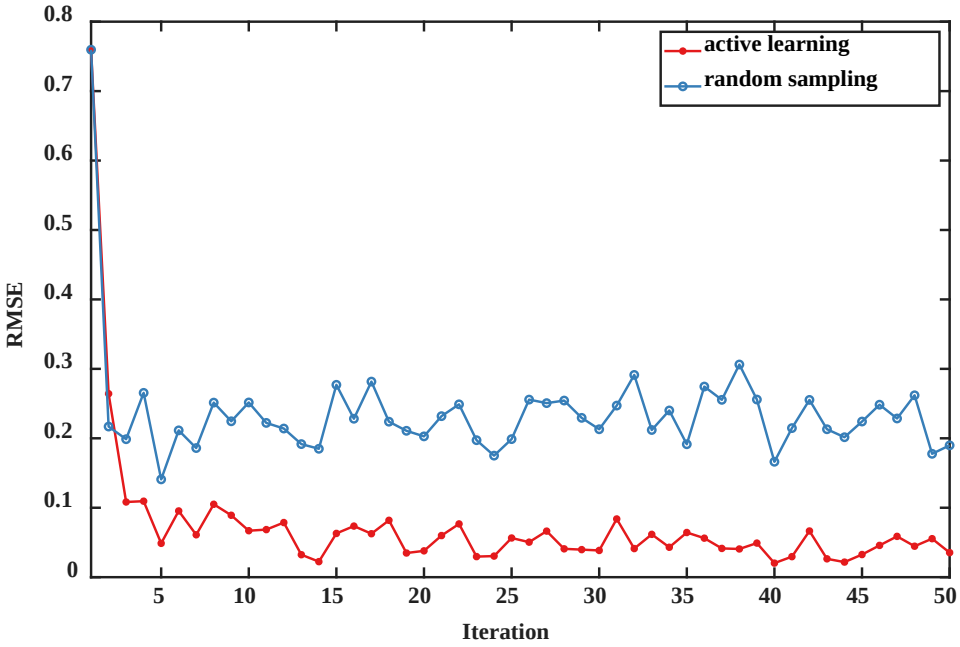

Fig. 11 The comparison of the effect of active learning and random sampling

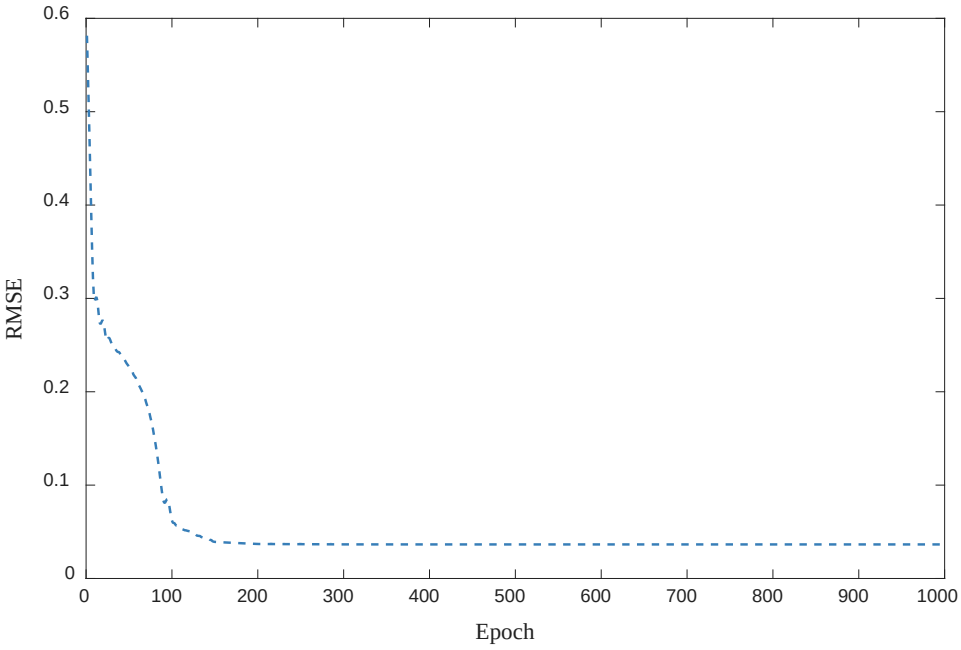

Fig. 12 Convergence of the loss function for the first GRU model

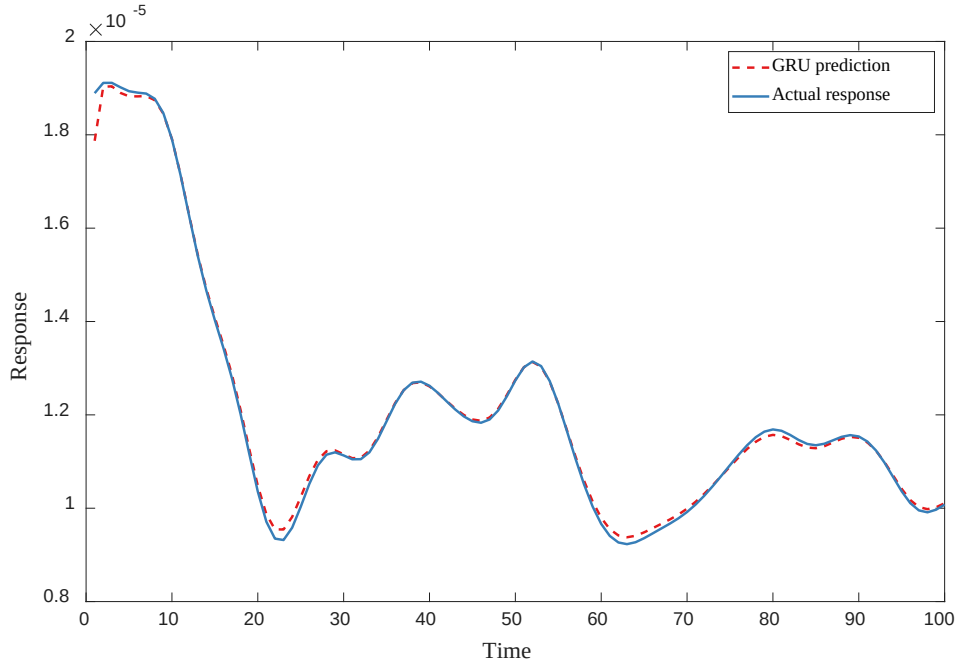

Fig. 13 Comparisons between actual responses and estimations from GRU models

For each GRU model, 5000 MCS samples of stochastic processes are fed into to obtain the responses of the conditional uncertain structure response functions as augmented data. Once all the augmented data have been collected from all GRU models,

GP models for modeling the time-variant response can be constructed as introduced in Sec. 3.3. Fig. 14 shows the comparison of the accurate and predicted time-variant responses with respect to the 100 th MCS samples, which further demonstrates that time-variant response predictions can be achieved accurately by utilizing the constructed GP models.

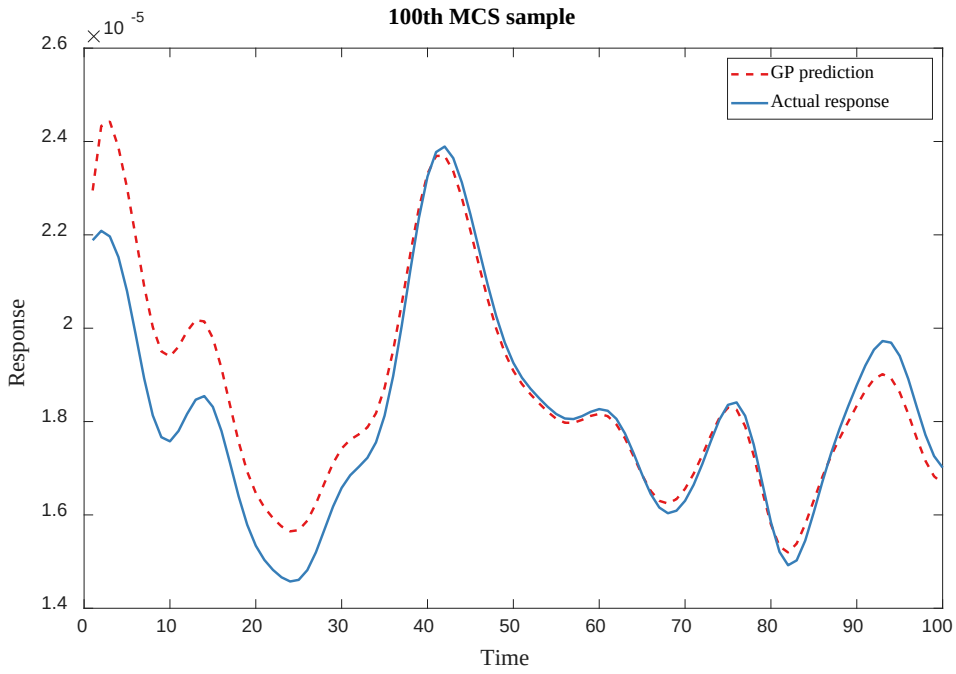

Fig. 14 Comparisons between the actual and estimated time-variant responses

To demonstrate the accuracy of the proposed approach, the direct MCS method is adopted as the reference solution. In the direct MCS method, the sampling number for random variables is 5000 and the sampling number for stochastic processes is also 5000, which means the total sampling number is 25000000. It can be seen from the Fig. 15 that the calculation results of the proposed approach are very consistent with the reference solutions calculated by the direct MCS method. Similarly, the RSM method is employed for comparison by utilizing the same number calls of the uncertain

structural response function. The average relative error rate of the mean of displacement at node 13 calculated by the proposed approach and RSM are 1.51% and 1.71%, respectively. As for the standard deviation of displacement at node 13, the average relative error rate calculated by the proposed approach and RSM are 2.34% and 12.75%, respectively. This further verifies that the proposed approach can be used for the response analysis of time-variant uncertain structures with mixed random variables and stochastic processes, and can obtain very good accuracy. In addition, compared with the calculation amount of 25000000 samplings of the direct MCS method, the proposed approach only needs 40 calculations of the uncertain structural response function to obtain the global surrogate model, which is very small. Its calculation efficiency is much higher than that of the direct MCS method.

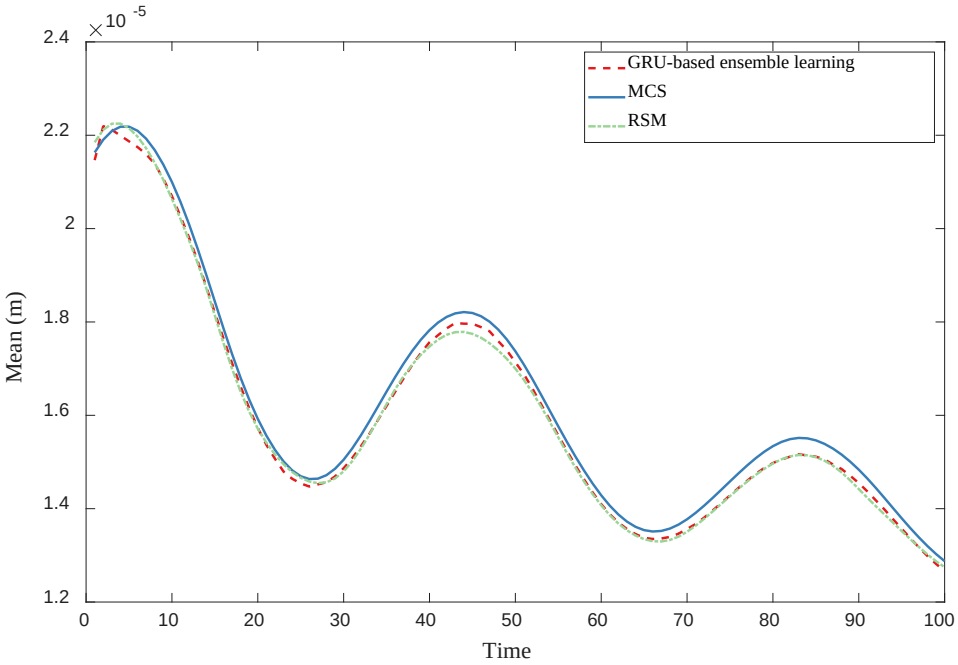

(a)

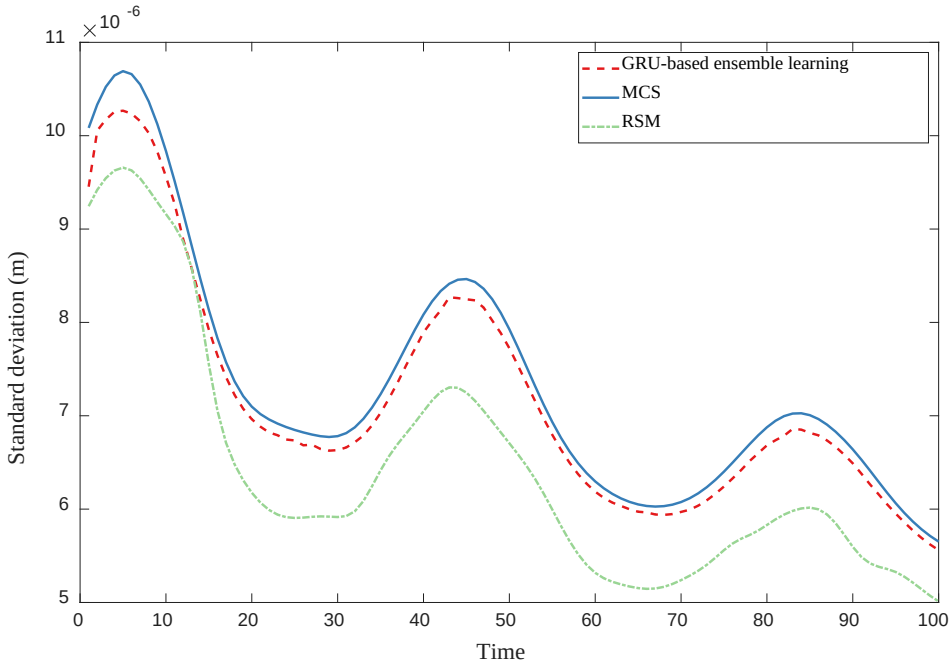

(b)

Fig. 15 The mean and standard deviation of displacement at node 13: (a) mean (b) standard deviation

5 Conclusion

In this paper, a GRU-based ensemble learning framework is proposed, where MCS is adopted for the response analysis of time-variant uncertain structures based on the combination of GRU networks and the GP modelling technique. By introducing the conditional uncertain structural response function, the GRU networks are employed to learn the relationship between stochastic processes and time-variant structural responses. Given one time-series data, a GRU model can be constructed, which can be well-trained and can accurately approximate the conditional uncertain structural response function. For multiple sets of time-independent random variables and time-dependent stochastic processes sampled by LHS, multiple GRU models can be obtained.

Based on the MCS samples of stochastic processes, the time-variant response predictions can be collected as augmented data through multiple trained GRU models. At a specific time instant, GP models are constructed to model the mapping relationship between random variables and time-variant structural responses after reorganizing the augmented data. As a result, time-variant structural response prediction can be calculated based on the GP models with respect to the MCS samples of random variables. Two engineering examples, including a plane truss structure and a continuum shell structure considering a mixed uncertainty model with random variable and stochastic process, verify the effectiveness of the proposed method. Numerical results demonstrate that the proposed approach can achieve both accuracy and efficiency. Moreover, the proposed approach is capable of accurately predicting the overall time-variant responses, even if the uncertainty of the time-variant structure is relative large. Compared with the direct MCS method, the computational burden of the GRU-based ensemble learning framework is much reduced due to the high computational efficiency of the GRU local surrogate model and the GP process global surrogate model. Thus, the GRU-based ensemble learning framework provides a good platform for the response analysis of time-variant uncertain structures.

Acknowledgement

The paper is supported by the National Natural Science Foundation of China (Grant No. 51905162), the Foundation for Innovative Research Groups of the National Natural Science Foundation of China (Grant No. 51621004) and the Fundamental Research Funds for the Central Universities (531107051148). The author would also like to thank

reviewers for their valuable suggestions.

References

[1] Doltsinis I , Zhan K . Perturbation-based stochastic FE analysis and robust design of inelastic deformation processes[J]. Computer Methods in Applied Mechanics & Engineering, 2006, 195(19/22):2231-2251.

[2] Ichchou M N , Bouchoucha F , Souf M , et al. Stochastic wave finite element for random periodic media through first-order perturbation[J]. Computer Methods in Applied Mechanics and Engineering, 2011, 200(41):2805-2813.

[3] Dash P, Singh B N. Geometrically nonlinear free vibration of laminated composite plate embedded with piezoelectric layers having uncertain material properties[J]. Journal of vibration and acoustics, 2012, 134(6).

[4] Adhikari S. Doubly spectral stochastic finite-element method for linear structural dynamics[J]. Journal of Aerospace Engineering, 2011, 24(3): 264-276.

[5] Yadav V, Rahman S. Uncertainty quantification of high‐dimensional complex systems by multiplicative polynomial dimensional decompositions[J]. International journal for numerical methods in engineering, 2013, 94(3): 221-247.

[6] Sarrouy E, Dessombz O, Sinou J J. Piecewise polynomial chaos expansion with an application to brake squeal of a linear brake system[J]. Journal of Sound and Vibration, 2013, 332(3): 577-594.

[7] Puig B, Poirion F, Soize C. Non-Gaussian simulation using Hermite polynomial expansion: convergences and algorithms[J]. Probabilistic Engineering Mechanics, 2002, 17(3): 253-264.

[8] Field Jr R V, Grigoriu M. On the accuracy of the polynomial chaos approximation[J]. Probabilistic Engineering Mechanics, 2004, 19(1-2): 65-80.

[9] Naess A, Gaidai O. Monte Carlo methods for estimating the extreme response of dynamical systems[J]. Journal of Engineering Mechanics, 2008, 134(8): 628-636.

[10] Saha N, Naess A. Monte–Carlo based method for predicting extreme value statistics of uncertain structures[J]. Journal of engineering mechanics, 2010, 136(12): 1491-1501.

[11] Seçgin A, Dunne J F, Zoghaib L. Extreme-value-based statistical bounding of low, mid, and high frequency responses of a forced plate with random boundary conditions[J]. Journal of vibration and acoustics, 2012, 134(2).

[12] Rajabalinejad M, Meester L E, Van Gelder P, et al. Dynamic bounds coupled with Monte Carlo simulations[J]. Reliability engineering & system safety, 2011, 96(2): 278-285.

[13] Hurtado J E, Alvarez D A. The encounter of interval and probabilistic approaches to structural reliability at the design point[J]. Computer Methods in Applied Mechanics and Engineering, 2012, 225: 74-94.

[14] Schuëller G I. Developments in stochastic structural mechanics[J]. Archive of Applied Mechanics, 2006, 75(10): 755-773.

[15] Schuëller G I, Pradlwarter H J, Koutsourelakis P S. A critical appraisal of reliability estimation procedures for high dimensions[J]. Probabilistic engineering mechanics, 2004, 19(4): 463-474.

[16] Koutsourelakis P S, Pradlwarter H J, Schuëller G I. Reliability of structures in high dimensions, part I: algorithms and applications[J]. Probabilistic Engineering Mechanics,

2004, 19(4): 409-417.

[17] Boyaval S, Lelievre T. A variance reduction method for parametrized stochastic differential equations using the reduced basis paradigm[J]. Communications in Mathematical Sciences, 2010, 8(3): 735-762.

[18] Boyaval S. A fast Monte–Carlo method with a reduced basis of control variates applied to uncertainty propagation and Bayesian estimation[J]. Computer Methods in Applied Mechanics and Engineering, 2012, 241: 190-205.

[19] Shinozuka M, Jan C M. Digital simulation of random processes and its applications[J]. Journal of sound and vibration, 1972, 25(1): 111-128.

[20] Cho H, Venturi D, Karniadakis G E. Karhunen–Loève expansion for multi-correlated stochastic processes[J]. Probabilistic Engineering Mechanics, 2013, 34: 157-167.

[21] Kim H, Shields M D. Modeling strongly non-Gaussian non-stationary stochastic processes using the iterative translation approximation method and Karhunen–Loève expansion[J]. Computers & Structures, 2015, 161: 31-42.

[22] Field Jr R V, Grigoriu M. On the accuracy of the polynomial chaos approximation[J]. Probabilistic Engineering Mechanics, 2004, 19(1-2): 65-80.

[23] Mao C, Jiang Y, Wang D, et al. Modeling and simulation of non-stationary vehicle vibration signals based on Hilbert spectrum[J]. Mechanical Systems and Signal Processing, 2015, 50: 56-69.

[24] Elishakoff I, Colombi P. Combination of probabilistic and convex models of uncertainty when scarce knowledge is present on acoustic excitation parameters[J]. Computer methods in applied mechanics and engineering, 1993, 104(2): 187-209.

[25] Wang C, Qiu Z. Hybrid uncertain analysis for steady-state heat conduction with

random and interval parameters[J]. International Journal of Heat and Mass Transfer, 2015, 80(jan.):319–328.

[26] Wang L, Ni B, Wang X, et al. Reliability-based Topology Optimization for Heterogeneous Composite Structures under Interval and Convex Mixed Uncertainties[J]. Applied Mathematical Modelling, 2021.

[27] Xia B, Yu D, Liu J. Hybrid uncertain analysis for structural–acoustic problem with random and interval parameters[J]. Journal of Sound and Vibration, 2013, 332(11): 2701-2720.

[28] Chen N , Xia S , Yu D , et al. Hybrid interval and random analysis for structural-acoustic systems including periodical composites and multi-scale bounded hybrid uncertain parameters[J]. Mechanical Systems & Signal Processing, 2019, 115(JAN.15):524-544.

[29] Zhu W , Chen N , Liu J , et al. A probability-box-based method for propagation of multiple types of epistemic uncertainties and its application on composite structural-acoustic system[J]. Mechanical Systems and Signal Processing, 2021, 149(2):107184.

[30] Jiang C , Liu N Y , Ni B Y . A Monte Carlo simulation method for non-random vibration analysis[J]. Acta Mechanica, 2017, 228(7):1-23.

[31] Xia B , Wang L . Non-probabilistic interval process analysis of time-varying uncertain structures[J]. Engineering Structures, 2018, 175:101-112.

[32] Chojaczyk A A, Teixeira A P, Neves L C, et al. Review and application of artificial neural networks models in reliability analysis of steel structures[J]. Structural Safety, 2015, 52: 78-89.

[33] Li M, Wang Z. An LSTM-Based Ensemble Learning Approach for Time-Dependent Reliability Analysis[J]. Journal of Mechanical Design, 2021, 143(3):

031702.

[34] Zhou T, Peng Y. Efficient reliability analysis based on deep learning-enhanced surrogate modelling and probability density evolution method[J]. Mechanical Systems and Signal Processing, 2022, 162: 108064.

[35] Xiang Z, Chen J, Bao Y, et al. An active learning method combining deep neural network and weighted sampling for structural reliability analysis[J]. Mechanical Systems and Signal Processing, 2020, 140: 106684.

[36] Minar M R , Naher J . Recent Advances in Deep Learning: An Overview[J]. 2018.

[37] Choi E, Schuetz A, Stewart W F, et al. Using recurrent neural network models for early detection of heart failure onset[J]. Journal of the American Medical Informatics Association, 2017, 24(2): 361-370.

[38] Guo L, Li N, Jia F, et al. A recurrent neural network based health indicator for remaining useful life prediction of bearings[J]. Neurocomputing, 2017, 240: 98-109.

[39] Chung J , Gulcehre C , Cho K H , et al. Empirical Evaluation of Gated Recurrent Neural Networks on Sequence Modeling[J]. Eprint Arxiv, 2014.

[40] Cho K , Merrienboer B V , Gulcehre C , et al. Learning Phrase Representations using RNN Encoder-Decoder for Statistical Machine Translation[J]. Computer Science, 2014.

[41] Box J F. Guinness, Gosset, Fisher, and small samples[J]. Statistical science, 1987: 45-52.